LEARNING FAST, LEARNING SLOW: A GENERAL CONTINUAL LEARNING METHOD BASED ON COMPLEMENTARY LEARNING SYSTEM

Anonymous authors
Paper under double-blind review

ABSTRACT

Humans excel at continually learning from an ever-changing environment whereas it remains a challenge for deep neural networks which exhibit catastrophic forgetting. The complementary learning system (CLS) theory suggests that the interplay between rapid instance-based learning and slow structured learning in the brain is crucial for accumulating and retaining knowledge. Here, we propose CLS-ER, a novel dual memory experience replay (ER) method which maintains short-term and long-term semantic memories that interact with the episodic memory. Our method employs an effective replay mechanism whereby new knowledge is acquired while aligning the decision boundaries with the semantic memories. CLS-ER does not utilize the task boundaries or make any assumption about the distribution of the data which makes it versatile and suited for "general continual learning". Our approach achieves state-of-the-art performance on standard benchmarks as well as more realistic general continual learning settings.

1 INTRODUCTION

Continual learning (CL) refers to the ability of a learning agent to continuously interact with a dynamic environment and process a stream of information to acquire new knowledge while consolidating and retaining previously obtained knowledge (Parisi et al., 2019). This ability to continuously learn from a changing environment is a hallmark of intelligence and a critical missing component in our quest towards making our models truly intelligent. The major challenge towards enabling CL in deep neural networks (DNNs) is that the continual acquisition of incrementally available information from non-stationary data distributions generally leads to catastrophic forgetting whereby the performance of the model on previously learned tasks drops drastically as it learns new tasks (McCloskey & Cohen, 1989).

Several approaches have been proposed to address the issue of catastrophic forgetting in CL. These can be broadly categorized into regularization-based methods (Farajtabar et al., 2020; Kirkpatrick et al., 2017; Ritter et al., 2018; Zenke et al., 2017) which penalizes changes in the network weights, network expansion-based methods (Rusu et al., 2016; Yoon et al., 2017) which dedicate a distinct set of network parameters to distinct tasks, and rehearsal-based methods (Chaudhry et al., 2018; Lopez-Paz & Ranzato, 2017) which maintains a memory buffer and replays samples from previous tasks. Amongst these, rehearsal-based methods have proven to be more effective in challenging CL tasks (Farquhar & Gal, 2018). However, an optimal approach for replaying memory samples and constraining the model update to efficiently consolidate knowledge remains an open question.

In the brain, the ability to continually acquire, consolidate, and transfer knowledge over time is mediated by a rich set of neurophysiological processing principles (Parisi et al., 2019; Zenke et al., 2017) and multiple memory systems (Hassabis et al., 2017). In particular, the CLS theory (Kumaran et al., 2016) posits that efficient learning requires two complementary learning systems: the hippocampus exhibits short-term adaptation and rapid learning of episodic information which is then gradually consolidated to the neocortex for slow learning of structured information. Furthermore, a recent study by Hayes et al. (2021) identified the missing elements of biological reply in the replay mechanisms employed in DNNs for CL. They highlight that many existing approaches only focus on modeling the prefrontal cortex directly and do not have a fast learning network which plays a critical

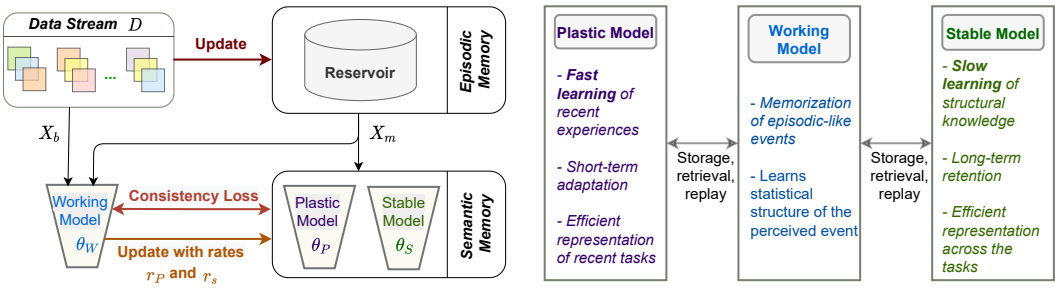

Figure 1: CLS-ER employs a dual-memory learning mechanism whereby the episodic memory stores the data samples and the semantic memories build the short-term and long-term memories of the learned semantic representations of the working model. The two memories interact to enforce a consistency loss on the working model which prevents rapid changes in the parameter space and enables the alignment of the decision boundary with semantic memories for effective knowledge consolidation.

role in enabling efficient CL in the brain. Inspired by these studies, we hypothesize that mimicking the slow and rapid adaptation of information and having an efficient mechanism for incorporating them into the working memory can enable better CL in DNNs.

To this end, we propose a novel dual memory experience replay method based on the complementary learning systems theory in the brain, dubbed as CLS-ER. In addition to a small episodic memory, our method builds long-term and short-term semantic memories which mimic the rapid and slow adaptation of information (Figure 1). As the network weights encode the learned representations of the tasks (Krishnan et al., 2019), the semantic memories are maintained by taking the exponential moving average of the working model's weights to consolidate information across the tasks with varying time windows and frequencies. The semantic memories interact with the episodic memory to extract consolidated replay activation patterns and enforce a consistency loss on the update of the working model so that new knowledge is acquired while aligning the decision boundary of the working model with the decision boundaries of semantic memories. This maintains a balance between the plasticity and stability of the model for effective knowledge consolidation.

CLS-ER provides a general CL method that does not utilize the task boundaries or make any strong assumption regarding the distribution of the data and tasks. We demonstrate the versatility and effectiveness of our method on a wide range of CL benchmark tasks as well as more challenging scenarios which simulate the complexities of CL in the real world.

2 Related Work

The base method for the rehearsal-based approach, Experience Replay (ER) (Riemer et al., 2018) combines the memory samples with the task samples into the training batch. Several techniques have since been employed on top of ER. Meta Experience Replay (MER) (Riemer et al., 2018) considers replay as a meta-learning problem for maximizing the transfer from previous tasks and minimizing the interference. iCARL (Rebuffi et al., 2017) uses the nearest average representation of past exemplars to classify in an incrementally learned representation space. Gradient Episodic Memory (GEM) (Lopez-Paz & Ranzato, 2017) formulates optimization constraints on the exemplars in memory. Gradient-based Sample Selection (GSS) (Aljundi et al., 2019) aims for memory sample diversity in the gradient space and provides a greedy selection approach. Function Distance Regularization (FDR) (Benjamin et al., 2018) saves the network response at the task boundaries and adds a consistency loss on top of ER. Dark Experience Replay (DER++) relaxes this restriction and samples logits during the entire optimization trajectory.

CLS has been used as a source of inspiration for dual memory learning systems in earlier works (French, 1999; Robins, 1993) but they have not been shown to scale to current computer vision benchmark datasets (Parisi et al., 2019). Recently, Rostami et al. (2019) utilizes a generative model to couple sequential tasks in a latent embedding space. Kamra et al. (2017) utilizes two generative models in a dual memory architecture. However, they utilize the task boundaries and generative

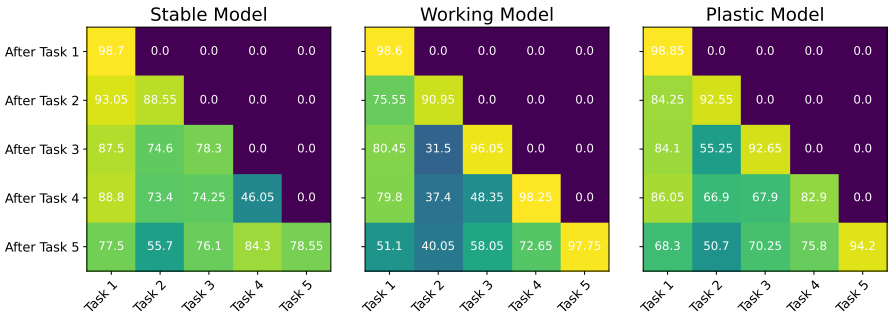

Figure 2: Task-wise performance for the individual models on S-CIFAR-10 test set with 500 buffer size. The models are evaluated at the end of each task (y-axis) to evaluate how the task performances (x-axis) are affected as training progress. The stable model retains information from earlier tasks while the plastic model quickly adapts to the recent task. Note that there is less forgetting in the semantic memories compared to the working model. For other buffer sizes and S-TinyImageNet see Figures S1 and S2 in Appendix.

replay has its own set of challenges as it is difficult to learn a faithful distribution and performs sub par in comparison to instance based replay methods on challenging CL settings. Generally, the inspiration from CLS theory in DNNs has been mostly limited to the use of episodic memory, and mimicking the rapid and slow learning mechanism is majorly ignored (Hayes et al., 2021) which our work aims to address.

3 Method

We first provide an overview of the complementary learning system theory for the brain and how we aim to mimic it for DNNs before introducing the main components of our method and the overall formulation.

3.1 Complementary Learning System Theory

The CLS theory posits that effective lifelong learning in the brain requires two complementary learning systems. The hippocampus rapidly encodes novel information as a short-term memory which is subsequently used to transfer and consolidate knowledge in the neocortex which gradually acquires structured knowledge representation as long-term memory through experience replay. The interplay between the functionality of hippocampus and neocortex is crucial for concurrently learning efficient representations (for better generalization) and the specifics of instance-based episodic memory.

3.2 Complementary Learning System based Experienced Replay

Inspired by the CLS theory, we propose a dual memory experience replay method, CLS-ER, which aims to mimic the interplay between fast learning and slow learning mechanisms for enabling effective CL in DNNs. Our method maintains short-term and long-term semantic memories of the encountered tasks which interact with the episodic memory for replaying the associated neural activities. The working model is updated so that it acquires new knowledge while aligning its decision boundary with the semantic memories to enable the consolidation of structured knowledge across the tasks. Figure 1 highlights the parallels between CLS theory and our method.

Semantic Memories: Central to our method is the maintenance of two semantic memories which accumulate and consolidate information over long-term and short-term periods. As the acquired knowledge of the learned tasks is encoded in the weights of DNNs (Krishnan et al., 2019), we aim to form our semantic memories by accumulating the knowledge encoded in the corresponding weights of the model as it sequentially learns different tasks.

An efficient method for aggregating the weights of a model is provided by *Mean Teacher* (Tarvainen & Valpola, 2017) which is a knowledge distillation approach that uses an exponential moving aver-

age (EMA) of the student's weights during training as the teacher for semi-supervised learning. It can also be considered as forming a self-ensemble of the intermediate model states that leads to better internal representations. We adapt the Mean Teacher approach to build our semantic memories as it provides a computational and memory-efficient method for accumulating knowledge over the tasks.

As CL involves learning tasks sequentially, the model weights at each training step can be considered as a student model specialized for a particular task. Therefore, averaging the weights during training can be considered as forming an ensemble of task-specific student models which effectively aggregates information across the tasks and leads to smoother decision boundaries. CLS-ER builds long-term (stable model) and short-term (plastic model) semantic memories by maintaining two EMA-weighted models over the working model's weights. The stable model is updated less frequently with a larger window size so that it retains more information from the earlier tasks while the plastic model is updated more frequently with a smaller window size so that it adapts faster to information from new tasks (Figure 2).

Episodic Memory: Replay of samples from the previous tasks stored in a small episodic memory is a common approach in CL that has proven to be effective in mitigating catastrophic forgetting. As we aim to position CLS-ER as a versatile general incremental learning method, we do not utilize the task boundaries or make any strong assumptions about the distribution of the tasks or samples. Therefore, to maintain the episodic memory buffer instead of the common task stratified sampling approach, we employ *reservoir sampling* (Vitter, 1985) which takes in a datastream of unknown length and assigns equal probability to each sample in the stream for being represented in the buffer. Reservoir sampling is a global distribution matching strategy that ensures that at any given time the distribution of samples in the buffer will approximately match the distribution of all the samples seen so far (Isele & Cosgun, 2018).

Consolidation of Information: The key challenge in CL is the consolidation of new information with the previously acquired information. This requires an effective balance between the stability and plasticity of the model. Furthermore, the sharp change in decision boundary as a new task is learned, makes the consolidation of information over tasks more challenging. CLS-ER tackles these challenges through a novel dual memory experience replay mechanism. The long-term and short-term semantic memories interact with the episodic memory to extract the consolidated activations for the memory samples which are then utilized to constrain the update of the working model so that new knowledge is obtained whilst the decision boundary is aligned with the semantic memories. This prevents rapid changes in the parameter space as new tasks are learned. Furthermore, aligning the working model's decision boundary with the semantic memories serves two goals: (i) helps in retaining and consolidating information and (ii) leads to a smoother adaptation of decision boundary.

3.3 Formulation

CLS-ER involves training a working model $f(.;\theta_w)$ on a data stream $\mathcal{D}$ sampled from a non-iid distribution. Two additional EMA-weighted models are maintained as semantic memories: plastic model $f(.;\theta_P)$ and the stable model $f(.;\theta_S)$. Finally, reservoir sampling (Vitter, 1985) is employed to maintain a small episodic memory $\mathcal{M}$.

At each training step, the working model receives the training batch X_b from the data stream and retrieves a random batch of exemplars X_m from the episodic memory. This is then followed by retrieval of semantic information about the exemplars from the two semantic memories (Figure 1). The semantic memories are designed so that the plastic model has higher performance on recent tasks whereas the stable model prioritizes retaining information on the older tasks. Therefore, we would prefer to use the logits from the stable model Z_S for older exemplars and the plastic model Z_P for recent exemplars. As CLS-ER is a general incremental learning method that does not utilize the task boundaries, instead of fixing some hard threshold on when to prefer one over the other or use the task information, we opt for the simple and task-agnostic approach of deciding based on the performance of the semantic memories on the exemplars which empirically works well. For each exemplar, we select the replay logits Z based on which model has the highest softmax score for the ground-truth class (line 5-6 in Algorithm 1).

The selected replay logits from the semantic memories are then used to enforce a consistency loss on the working model so that it does not deviate from the already learned experiences. Hence, the

Algorithm 1 Complementary Learning System-Experience Replay Algorithm

Input: Data stream $\mathcal{D}$, Learning rate η, Consistency weight λ, Update rates r_P and r_S, Decay parameters α_P and α_S
Initialize: $\theta_W = \theta_P = \theta_S$
$\mathcal{M} \leftarrow \{\}$
while Training **do**
  $(X_b, Y_b) \sim \mathcal{D}$
  $(X_m, Y_m) \sim \mathcal{M}$
  $(X, Y) = \{(X_b, Y_b), (X_m, Y_m)\}$
  $Z_P, Z_S \leftarrow f(X_m; \theta_P), f(X_m; \theta_S)$ ▷ Select optimal semantic memory
  $Z \leftarrow Z_P$ **if** $\sigma(Z_P)^{(Y_m)} > \sigma(Z_S)^{(Y_m)}$ **else** Z_S
  $\mathcal{L} = \mathcal{L}_{CE}(\sigma(f(X; \theta_W)), Y) + \lambda \mathcal{L}_{MSE}(f(X_m; \theta_W), Z)$ ▷ Update working model
  $\theta_W \leftarrow \theta_W - \eta \nabla_{\theta_W} \mathcal{L}$
  $a, b \sim \mathcal{U}(0, 1)$ ▷ Update semantic memories
  $\theta_P \leftarrow \alpha_p \theta_P + (1 - \alpha_P)\theta_W$ **if** $a < r_P$ **else** θ_P
  $\theta_S \leftarrow \alpha_S \theta_S + (1 - \alpha_S)\theta_W$ **if** $b < r_S$ **else** θ_S
  $\mathcal{M} \leftarrow Reservoir(\mathcal{M}, (X_b, Y_b))$ ▷ Update episodic memory
return $\theta_W, \theta_P, \theta_S$

working model is updated with a combination of the cross-entropy loss on the union of the data stream and episodic memory samples, X, and the consistency loss on the exemplars X_m;

$$\mathcal{L} = \mathcal{L}_{CE}(\sigma(f(X; \theta_W)), Y) + \lambda \mathcal{L}_{MSE}(f(X_m; \theta_W), Z) \tag{1}$$

where σ is the softmax function, λ the regularization parameter, and $\mathcal{L}_{MSE}$ the mean squared error loss used as consistency term.

After updating the working model, we stochastically update the plastic and stable models with rates r_P and r_S (note that $r_P \geq r_S$ so that the plastic model is updated more frequently). The semantic memories are updated by taking an exponential moving average of the working model's weights (Tarvainen & Valpola, 2017) with decay parameters α_P and α_S, respectively.

$$\theta_i = \alpha_i \theta_i + (1 - \alpha_i)\theta_W, \quad i \in \{P, S\} \tag{2}$$

Note that $\alpha_P \leq \alpha_S$ so that the plastic model mimics the rapid adaptation of information while the stable model mimics slow acquisition of structured knowledge.

For inference, we use the stable model as it retains long-term memory across the tasks, consolidates structural knowledge, and learns efficient representations for generalization (Figure 1). Details of our proposed method are provided in Algorithm 1.

4 Experimental Setup

To ensure a fair comparison of different CL methods under uniform experimental settings, we extended the Mammoth framework provided by Buzzega et al. (2020a) and unless stated otherwise, we follow the same training scheme (learning rate, batch sizes of incoming data and memory buffer, and the number of training epochs) as them for each of the evaluation settings. To find the optimal hyperparameters for CLS-ER, we run a grid search over λ, α_S, α_P, r_S, and r_P on a small validation set. Section C.2 and B.5 in Appendix show that our method is not highly sensitive to the particular choice of hyperparameters and different settings can attain similar performance. Also, because of the complementary nature of the components, we can often fix a set of parameters (e.g. λ, α_S, α_P and r_S) and only finetune the remaining parameters (e.g. r_P) which facilitates hyperparameter tuning significantly.

Following Buzzega et al. (2020a), we employ a fully connected network with two hidden layers, each with 100 ReLU units on all the variants of the MNIST dataset and ResNet-18 (He et al., 2015) network without pretraining for the other datasets. In all of our settings, we use the Stochastic Gradient Descent optimizer. We use random horizontal flip and random crop on both the stream and buffer samples for S-CIFAR-10, S-Tiny-ImageNet, and GCIL-CIFAR-100. The selected hyperparameters for each of the settings are provided in Table S4 in Appendix. Note that for the vast majority of

Buffer	Method	Class-IL			Domain-IL
		S-MNIST	S-CIFAR-10	S-Tiny-ImageNet	R-MNIST
–	JOINT	95.57±0.24	92.20±0.15	59.99±0.19	95.76±0.04
	SGD	19.60±0.04	19.62±0.05	7.92±0.26	67.66±8.53
200	ER	80.43±1.89	44.79±1.86	8.49±0.16	85.01±1.90
	GEM	80.11±1.54	25.54±0.76	-	80.80±1.15
	iCaRL	70.51±0.53	49.02±3.20	7.53±0.79	-
	FDR	79.43±3.26	30.91±2.74	8.70±0.19	85.22±3.35
	GSS	38.92±2.49	39.07±5.59	-	79.50±0.41
	DER++	85.61±1.40	64.88±1.17	10.96±1.17	90.43±1.87
	CLS-ER	**89.54±0.21**	**66.19±0.75**	**21.95±0.26**	**92.26±0.18**
500	ER	86.12±1.89	57.74±0.27	9.99±0.29	88.91±1.44
	GEM	85.99±1.35	26.20±1.26	-	81.15±1.98
	iCaRL	70.10±1.08	47.55±3.95	9.38±1.53	-
	FDR	85.87±4.04	28.71±3.23	10.54±0.21	89.67±1.63
	GSS	49.76±4.73	49.73±4.78	-	81.58±0.58
	DER++	91.00±1.49	72.70±1.36	19.38±1.41	92.77±1.05
	CLS-ER	**92.05±0.32**	**75.22±0.71**	**29.61±0.54**	**94.06±0.07**
5120	ER	93.40±1.29	19.70±0.07	28.97±0.41	94.19±0.44
	GEM	95.11±0.87	67.27±4.27	-	85.24±0.59
	iCaRL	70.60±1.03	55.07±1.55	14.08±1.92	-
	FDR	87.47±3.15	19.70±0.07	28.97±0.41	94.19±0.44
	GSS	89.39±0.75	67.27±4.27	-	85.24±0.59
	DER++	95.30±1.20	85.24±0.49	39.02±0.97	**94.65±0.33**
	CLS-ER	**95.73±0.11**	**86.78±0.17**	**45.92±0.30**	94.25±0.06

Table 1: Comparison with prior works on Class-IL and Domain-IL settings. The baseline results are from Buzzega et al. (2020a) (- indicates the experiments that the authors were unable to run) and following them, we report the mean and one standard deviation over 10 runs.

datasets, we use uniform settings (lr, epochs, batch size, memory batch size, and $lambda$) across the different buffer sizes and requires only slight modifications in the other hyperparameters which shows that our method does not require extensive finetuning for different memory budgets. For each of our experiments, we fix the order of the classes and report the average and one standard deviation of the mean test accuracy of all the tasks across 10 runs with different initializations. Section C in Appendix provides further implementation details.

5 Empirical Evaluation

There are a plethora of evaluation protocols in the CL literature, each of which biases the evaluation towards a certain approach (Farquhar & Gal, 2018; Mi et al., 2020; van de Ven & Tolias, 2019). It is therefore of utmost importance to conduct an extensive and robust evaluation over different CL settings to gauge the versatility of the method. Details of the datasets used in each CL setting is provided in section A in Appendix. We compare our method with the state-of-the-art rehearsal-based approaches on various CL settings and memory budgets under uniform experimental settings. *SGD* refers to standard training and *JOINT* provides an upper bound given by training all tasks jointly.

Class Incremental Learning (Class-IL): refers to the CL scenario where new classes are added with each subsequent task and the agent must learn to distinguish not only amongst the classes within the current task but also across previous tasks. Class-IL measures how well the method can learn general representations, accumulate, consolidate, and transfer the acquired knowledge to learn efficient representations and decision boundaries for all the classes seen so far.

Table 1 provides the comparison with six rehearsal-based approaches on Class-IL settings with varying datasets and task length complexities. CLS-ER provides the highest performance in all of these scenarios. In particular, as the dataset complexity and number of tasks increase from S-MNIST to S-Tiny-ImageNet, the performance gap between CLS-ER and DER++ increases considerably. Especially, with a smaller memory budget, CLS-ER is able to retain more information than other

JOINT	SGD	Buffer	ER	MER	GSS	DER++	CLS-ER
82.98±3.24	19.09±0.69	200	49.27±2.25	48.58±1.07	43.92±2.43	54.16±3.02	**66.37±0.83**
		500	65.04±1.53	62.21±1.36	54.45±3.14	69.62±1.59	**75.70±0.41**
		1000	75.18±1.50	70.91±0.76	63.84±2.09	76.03±1.61	**79.54±0.34**

Table 2: Comparison with prior works on MNIST-360 test set. The baseline results are from Buzzega et al. (2020a) and following them, we report the mean and one standard deviation over 10 runs.

Distribution	**Uniform**			**Longtail**		
SGD	18.05±5.01			15.02±6.07		
JOINT	60.19±1.21			54.72±7.60		
Buffer	200	500	1000	200	500	1000
ER	24.20±3.12	27.65±2.42	32.89±2.47	21.56±3.70	24.79±4.18	32.25±3.00
DER++	28.79±3.57	33.14±3.13	40.51±2.62	25.27±4.24	32.59±2.83	36.97±3.78
CLS-ER	**33.15±2.83**	**37.01±1.67**	**41.09±1.58**	**29.57±3.87**	**33.26±3.66**	**39.21±3.46**

Table 3: Comparison with prior works on GCIL-CIFAR-100 dataset. We ran all the methods for 10 runs and report the mean and one standard deviation.

rehearsal-based methods. In the most challenging setting, S-Tiny-ImageNet with 200 buffer size, CLS-ER provides a percentage gain of 163% and 104% over the baseline ER and the current state-of-the-art DER++, respectively. The results demonstrate the capability of CLS-ER to efficiently accumulate and retain knowledge over longer sequences under complex and memory restrictive scenarios.

We believe that the performance gains over DER++ highlight a key component of an efficient CL agent: the ability to consolidate previously acquired knowledge. DER++ fails to account for the consolidation of feature space and adaptation of the decision boundaries of the previous tasks. Therefore, constraining the model to match the sub-optimal logits might hamper the consolidation of knowledge. This becomes more prominent as the number of classes in each task, the sequence length, and the cross-task resemblance increase. For instance, for DER++, replaying a sample from Task-1 when training on S-Tiny-ImageNet Task-10, the reference logit values which are used to enforce the consistency are from a model representation state which has not considered how to distinguish the 20 classes in Task-1 from 80 additional classes which are visually and semantically similar. It stands to reason that the optimal representation space and subsequently the decision boundaries for the classes in Task-1 would drift considerably when required to distinguish between 80 additional classes as well. Therefore, the local information provided by the sub-optimal saved logits in DER++ fails to provide the global context required for consolidating knowledge. CLS-ER, on the other hand, extracts logits from the semantic memories which consolidate knowledge across the tasks, and hence the working model receives more optimal feedback.

Domain Incremental Learning (Domain-IL): refers to the CL scenario where the classes remain the same in each subsequent task but the input distribution changes. Table 1 shows that similar to Class-IL, we see performance gains with CLS-ER, particularly for lower memory budget. On 5120 buffer size, CLS-ER performs on par with the state-of-the-art DER++ method. The soft targets provide relational information about the classes for maintaining the similarity structure across the sequences. While the dataset complexity is low for R-MNIST, it involves a larger number of tasks with high cross-task resemblance. We, therefore, observe similar benefits of extracting replay logits from the consolidated semantic memories which provide feedback from a global context compared to the local information in DER++.

General Incremental Learning (GIL): Class-IL and Domain-IL fail to assimilate the challenges in the real world setting where the task boundaries are blurry, and classes can reappear and have different distributions. The CL method has to consider the sample efficiency, challenge of imbalanced data, and efficient knowledge transfer in addition to preventing catastrophic forgetting. We consider two GIL protocols: MNIST-360 (Buzzega et al., 2020a) exposes the model to both sharp (changes in class) and smooth (rotation of digits) distribution shifts. The Generalized Class Incremental Learning (GCIL) (Mi et al., 2020) is the closest to real-world scenario as it utilizes probabilistic modeling to sample the classes and data distributions in each task. The number of classes in each task is not fixed, the classes can overlap and the sample size for each class can vary.

Table 2 shows that CLS-ER provides considerable performance gains on the challenging MNIST-360, particularly with a low memory budget. Similarly, Table 3 demonstrates the effectiveness of CLS-ER on GCIL-CIFAR-100 under both uniform and imbalanced class samples. Both of these settings involve recurring classes in subsequent sequences which makes the transfer of knowledge from previous occurrences important. The performance gap between CLS-ER and DER++ in the recurring classes setting alludes to another shortcoming of saving logits from the previous state. Consider the case where class c appears in sequence (Seq)-1 with 20 samples, and then subsequently in Seq-5 with 200 samples. In the following sequences, DER++ uses exemplars from class c saved in Seq-1 with sub-optimal logits from the model state which was attained with only 20 samples and fails to take advantage of the better learned representations with additional data in Seq-5. CLS-ER, on the other hand, is able to take advantage of the additional samples and provide feedback from the improved learned representations.

6 Model Characteristics

We analyze CLS-ER and provide some insights into the characteristics of the proposed approach which enables it to learn effectively under challenging CL scenarios. In our subsequent analysis, we compare CLS-ER with the baseline ER and DER++.

6.1 Convergence to Flatter Minima

Due to the non-convexity of the loss landscape, there can be multiple solutions to the optimization objective, however, the local geometry at the convergence point can affect the generalization of the model. Solutions that reside in wide valleys instead of narrow crevices generalize better (Chaudhari et al., 2019; Keskar et al., 2016) as the predictions do not change drastically with small perturbations. A CL model which converges to flatter minima has more flexibility to explore the neighboring parameter space to optimize on the new task without drastically increasing the loss on the previous tasks. Following the analysis in Zhang et al. (2018), we add independent Gaussian noise of increasing strength to the parameters of the trained model and analyze the change in accuracy and loss across the training samples. Figure 3 shows that CLS-ER is significantly less sensitive to perturbations compared to ER and DER++. CLS-ER also retains performance for a longer period and its performance drops more smoothly. These results suggest that the fast and slow adaptation of information in CLS-ER can guide the optimization to wider valleys.

6.2 Task Probabilities

Because of the sequential nature of CL, an implicit bias is induced towards the current task (Wu et al., 2019). A number of CL methods employ explicit techniques to reduce this bias (Hou et al., 2019; Wu et al., 2019), however, they utilize the task boundaries which is counterproductive for general incremental learning. We believe that the efficient knowledge consolidation in CLS-ER through the semantic memories can implicitly mitigate the bias towards recent tasks. We follow the analysis performed in Buzzega et al. (2020b) to observe the probability of each task being predicted at the end of the training. For each sample in the test dataset, we take the softmax output and then average the probabilities of the associated classes for each task across the dataset. We normalize the values and report the probability of each task being predicted. Figure 3 (right plot) shows that CLS-ER is able to maintain a more uniform prediction probability across all the tasks over a long sequence. Figures S3 and S4 in Appendix shows similar results for other buffer sizes and S-TinyImageNet.

6.3 Model Calibration

Model calibration refers to the accuracy with which the scores provided by the model reflect its predictive uncertainty. The class probabilities predicted by DNNs are uncalibrated, often tending towards over-confidence which is detrimental to the reliability of the model's prediction (Guo et al., 2017). This is even more pronounced in CL where the models tend to be biased towards recent tasks. Following Guo et al. (2017), we provide the reliability diagrams (model accuracy as a function of it's prediction confidence) and the Expected Calibration Error (ECE; a weighted average over the absolute difference between accuracy and confidence). Figure 4 shows the remarkable ability of CLS-ER to provide well-calibrated models without the application of any calibration technique.

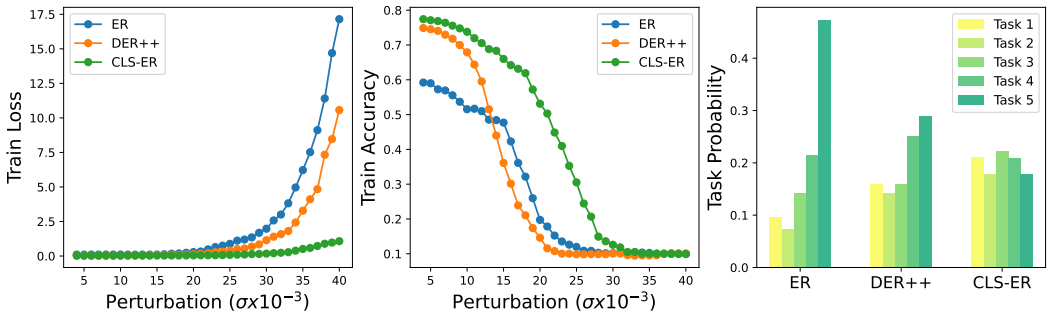

Figure 3: Model characteristics analyses of different methods trained on S-CIFAR-10 with 500 buffer size. The Left and middle figures show the training loss and accuracy under varying Gaussian noise added to the weights of each layer of the model. CLS-ER is considerably less sensitive to perturbations, suggesting convergence to flatter minima. The right figure shows the task probabilities. CLS-ER effectively mitigates the bias to the recent tasks and provides a more uniform probability of being predicted for the classes over the tasks even very early ones.

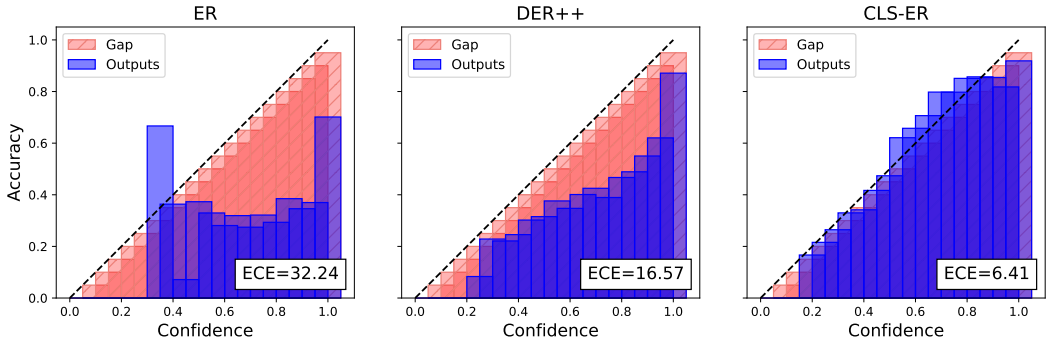

Figure 4: Reliability plots for different methods on S-CIFAR-10 with 500 buffer size. CLS-ER results in considerably better-calibrated models and hence more reliable predictions. For other buffer sizes and S-TinyImageNet see Figures S5 and S6 in Appendix.

Note that these characteristics are complementary in nature: convergence to flatter minima allows our method to remain in the vicinity of optimal parameters for previous tasks when adapting to the new task, this leads to more uniform performance across tasks which can improve the task probabilities, and since the model is not too biased towards the current task, the model can provide reliable prediction across the tasks which improve the calibration. Additional characteristics analyses on different datasets and buffer sizes are provided in Appendix. We observe that our model's behavior is consistent across varying datasets and buffer sizes.

7 Conclusion

We proposed a novel dual memory experience replay method based on the complementary learning systems theory in the brain. Our method maintains long-term and short-term semantic memories which are utilized to effectively replay the neural activities of the episodic memories and align the decision boundary of the working model for efficient knowledge consolidation. We demonstrated the effectiveness of our approach on benchmark datasets as well as more challenging general incremental learning scenarios and achieved the new state-of-the-art in the vast majority of the continual learning settings. We further showed that CLS-ER converges to flatter minima, mitigates the bias towards recent tasks, and provides a well-calibrated high-performance model. Our strong empirical results motivate further study into mimicking the complementary learning system in the brain more faithfully to enable optimal continual learning in DNNs.

REFERENCES

Rahaf Aljundi, Min Lin, Baptiste Goujaud, and Yoshua Bengio. Gradient based sample selection for online continual learning. In *Advances in Neural Information Processing Systems*, pp. 11816–11825, 2019. 2

Ari S Benjamin, David Rolnick, and Konrad Kording. Measuring and regularizing networks in function space. *arXiv preprint arXiv:1805.08289*, 2018. 2

Pietro Buzzega, Matteo Boschini, Angelo Porrello, Davide Abati, and Simone Calderara. Dark experience for general continual learning: a strong, simple baseline. *arXiv preprint arXiv:2004.07211*, 2020a. 5, 6, 7, 13, 14, 18, 19

Pietro Buzzega, Matteo Boschini, Angelo Porrello, and Simone Calderara. Rethinking experience replay: a bag of tricks for continual learning. *arXiv preprint arXiv:2010.05595*, 2020b. 8

Pratik Chaudhari, Anna Choromanska, Stefano Soatto, Yann LeCun, Carlo Baldassi, Christian Borgs, Jennifer Chayes, Levent Sagun, and Riccardo Zecchina. Entropy-sgd: Biasing gradient descent into wide valleys. *Journal of Statistical Mechanics: Theory and Experiment*, 2019(12): 124018, 2019. 8

Arslan Chaudhry, Marc'Aurelio Ranzato, Marcus Rohrbach, and Mohamed Elhoseiny. Efficient lifelong learning with a-gem. *arXiv preprint arXiv:1812.00420*, 2018. 1

Matthias De Lange, Rahaf Aljundi, Marc Masana, Sarah Parisot, Xu Jia, Ales Leonardis, Gregory Slabaugh, and Tinne Tuytelaars. A continual learning survey: Defying forgetting in classification tasks. *arXiv preprint arXiv:1909.08383*, 2019. 13

Mehrdad Farajtabar, Navid Azizan, Alex Mott, and Ang Li. Orthogonal gradient descent for continual learning. In *International Conference on Artificial Intelligence and Statistics*, pp. 3762–3773. PMLR, 2020. 1

Sebastian Farquhar and Yarin Gal. Towards robust evaluations of continual learning. *arXiv preprint arXiv:1805.09733*, 2018. 1, 6, 13, 14

Robert M French. Catastrophic forgetting in connectionist networks. *Trends in cognitive sciences*, 3(4):128–135, 1999. 2

Chuan Guo, Geoff Pleiss, Yu Sun, and Kilian Q Weinberger. On calibration of modern neural networks. In *International Conference on Machine Learning*, pp. 1321–1330. PMLR, 2017. 8

Demis Hassabis, Dharshan Kumaran, Christopher Summerfield, and Matthew Botvinick. Neuroscience-inspired artificial intelligence. *Neuron*, 95(2):245–258, 2017. 1

Tyler L Hayes, Giri P Krishnan, Maxim Bazhenov, Hava T Siegelmann, Terrence J Sejnowski, and Christopher Kanan. Replay in deep learning: Current approaches and missing biological elements. *arXiv preprint arXiv:2104.04132*, 2021. 1, 3

Kaiming He, Xiangyu Zhang, Shaoqing Ren, and Jian Sun. Deep residual learning for image recognition. corr abs/1512.03385 (2015), 2015. 5

Saihui Hou, Xinyu Pan, Chen Change Loy, Zilei Wang, and Dahua Lin. Learning a unified classifier incrementally via rebalancing. In *Proceedings of the IEEE/CVF Conference on Computer Vision and Pattern Recognition*, pp. 831–839, 2019. 8

David Isele and Akansel Cosgun. Selective experience replay for lifelong learning. In *Proceedings of the AAAI Conference on Artificial Intelligence*, volume 32, 2018. 4

Nitin Kamra, Umang Gupta, and Yan Liu. Deep generative dual memory network for continual learning. *arXiv preprint arXiv:1710.10368*, 2017. 2

Nitish Shirish Keskar, Dheevatsa Mudigere, Jorge Nocedal, Mikhail Smelyanskiy, and Ping Tak Peter Tang. On large-batch training for deep learning: Generalization gap and sharp minima. *arXiv preprint arXiv:1609.04836*, 2016. 8

J Kirkpatrick, R Pascanu, N Rabinowitz, J Veness, G Desjardins, AA Rusu, K Milan, J Quan, T Ramalho, A Grabska-Barwinska, et al. Overcoming catastrophic forgetting in neural networks.(dec. *arXiv preprint cs.LG/1612.00796*, 2016. 13

James Kirkpatrick, Razvan Pascanu, Neil Rabinowitz, Joel Veness, Guillaume Desjardins, Andrei A Rusu, Kieran Milan, John Quan, Tiago Ramalho, Agnieszka Grabska-Barwinska, et al. Overcoming catastrophic forgetting in neural networks. *Proceedings of the national academy of sciences*, 114(13):3521–3526, 2017. 1

Giri P Krishnan, Timothy Tadros, Ramyaa Ramyaa, and Maxim Bazhenov. Biologically inspired sleep algorithm for artificial neural networks. *arXiv preprint arXiv:1908.02240*, 2019. 2, 3

Alex Krizhevsky et al. Learning multiple layers of features from tiny images. 2009. 13

Dharshan Kumaran, Demis Hassabis, and James L McClelland. What learning systems do intelligent agents need? complementary learning systems theory updated. *Trends in cognitive sciences*, 20 (7):512–534, 2016. 1

Yann LeCun, Léon Bottou, Yoshua Bengio, and Patrick Haffner. Gradient-based learning applied to document recognition. *Proceedings of the IEEE*, 86(11):2278–2324, 1998. 13

David Lopez-Paz and Marc'Aurelio Ranzato. Gradient episodic memory for continual learning. In *Advances in neural information processing systems*, pp. 6467–6476, 2017. 1, 2, 13

Michael McCloskey and Neal J Cohen. Catastrophic interference in connectionist networks: The sequential learning problem. In *Psychology of learning and motivation*, volume 24, pp. 109–165. Elsevier, 1989. 1

Fei Mi, Lingjing Kong, Tao Lin, Kaicheng Yu, and Boi Faltings. Generalized class incremental learning. In *Proceedings of the IEEE/CVF Conference on Computer Vision and Pattern Recognition Workshops*, pp. 240–241, 2020. 6, 7, 13, 19

German I Parisi, Ronald Kemker, Jose L Part, Christopher Kanan, and Stefan Wermter. Continual lifelong learning with neural networks: A review. *Neural Networks*, 113:54–71, 2019. 1, 2

Hadi Pouransari and Saman Ghili. Tiny imagenet visual recognition challenge. *CS231N course, Stanford Univ., Stanford, CA, USA*, 2015. 13

Sylvestre-Alvise Rebuffi, Alexander Kolesnikov, Georg Sperl, and Christoph H Lampert. icarl: Incremental classifier and representation learning. In *Proceedings of the IEEE conference on Computer Vision and Pattern Recognition*, pp. 2001–2010, 2017. 2

Matthew Riemer, Ignacio Cases, Robert Ajemian, Miao Liu, Irina Rish, Yuhai Tu, and Gerald Tesauro. Learning to learn without forgetting by maximizing transfer and minimizing interference. *arXiv preprint arXiv:1810.11910*, 2018. 2

Hippolyt Ritter, Aleksandar Botev, and David Barber. Online structured laplace approximations for overcoming catastrophic forgetting. In *Advances in Neural Information Processing Systems*, pp. 3738–3748, 2018. 1

Anthony Robins. Catastrophic forgetting in neural networks: the role of rehearsal mechanisms. In *Proceedings 1993 The First New Zealand International Two-Stream Conference on Artificial Neural Networks and Expert Systems*, pp. 65–68. IEEE, 1993. 2

Mohammad Rostami, Soheil Kolouri, and Praveen K Pilly. Complementary learning for overcoming catastrophic forgetting using experience replay. *arXiv preprint arXiv:1903.04566*, 2019. 2

Andrei A Rusu, Neil C Rabinowitz, Guillaume Desjardins, Hubert Soyer, James Kirkpatrick, Koray Kavukcuoglu, Razvan Pascanu, and Raia Hadsell. Progressive neural networks. *arXiv preprint arXiv:1606.04671*, 2016. 1

Dongsub Shim, Zheda Mai, Jihwan Jeong, Scott Sanner, Hyunwoo Kim, and Jongseong Jang. Online class-incremental continual learning with adversarial shapley value. *arXiv e-prints*, pp. arXiv–2009, 2020. 13

Antti Tarvainen and Harri Valpola. Mean teachers are better role models: Weight-averaged consistency targets improve semi-supervised deep learning results. *arXiv preprint arXiv:1703.01780*, 2017. 3, 5

Gido M van de Ven and Andreas S Tolias. Three scenarios for continual learning. *arXiv preprint arXiv:1904.07734*, 2019. 6, 13

Jeffrey S Vitter. Random sampling with a reservoir. *ACM Transactions on Mathematical Software (TOMS)*, 11(1):37–57, 1985. 4

Yue Wu, Yinpeng Chen, Lijuan Wang, Yuancheng Ye, Zicheng Liu, Yandong Guo, and Yun Fu. Large scale incremental learning. In *Proceedings of the IEEE/CVF Conference on Computer Vision and Pattern Recognition*, pp. 374–382, 2019. 8

Jaehong Yoon, Eunho Yang, Jeongtae Lee, and Sung Ju Hwang. Lifelong learning with dynamically expandable networks. *arXiv preprint arXiv:1708.01547*, 2017. 1

Friedemann Zenke, Ben Poole, and Surya Ganguli. Continual learning through synaptic intelligence. *Proceedings of machine learning research*, 70:3987, 2017. 1, 13

Ying Zhang, Tao Xiang, Timothy M Hospedales, and Huchuan Lu. Deep mutual learning. In *Proceedings of the IEEE Conference on Computer Vision and Pattern Recognition*, pp. 4320–4328, 2018. 8

A CONTINUAL LEARNING SETTINGS

There is a plethora of evaluation protocols in the CL literature, each of which biases the evaluation towards a certain approach (Farquhar & Gal, 2018; Mi et al., 2020; Shim et al., 2020; van de Ven & Tolias, 2019). It is therefore of utmost importance to conduct an extensive and robust evaluation to gauge the versatility of the method. We believe that adhering to the key desiderata as suggested in Farquhar & Gal (2018) would help the CL community immensely in moving towards robust evaluation of methods. An experimental protocol which trains the method on a long sequence of tasks where the boundaries between the tasks are not distinct and the tasks themselves are not disjoint and the method does not make sure of task boundaries during training or testing can be considered as adhering to all five desiderata. Our work focuses on the aforementioned setting which can be considered as General Incremental Learning (GIL) setting. Here, we provide a broad categorization of these evaluation protocols which test different aspects of CL.

A.1 CLASS INCREMENTAL LEARNING (CLASS-IL)

Class-IL refers to the CL scenario where new classes are added with each subsequent task and the agent must learn to distinguish not only amongst the classes within the current task but also across previous tasks. Class-IL measures how well the method can learn general representations, accumulate, consolidate, and transfer the acquired knowledge to learn efficient representations and decision boundaries for all the classes seen so far. Following (Buzzega et al., 2020a; De Lange et al., 2019; Zenke et al., 2017), we consider the common benchmark datasets MNIST (LeCun et al., 1998) (**S-MNIST**), CIFAR-10 (Krizhevsky et al., 2009) (**S-CIFAR-10**) and Tiny-ImageNet (Pouransari & Ghili, 2015) (**S-Tiny-ImageNet**) which are split into 5, 5, and 10 tasks each including 2, 2, and 20 classes respectively. These represent Class-IL settings of increasing dataset complexity as well as longer sequences. While it is an important and challenging benchmark, it assumes that each subsequent task will have the same number of disjoint classes and have uniform samples for each class which is not representative of real-world scenarios. We do not consider the related Task Increment Learning (Task-IL) setting as it assumes the availability of task labels at both training and inference which cannot truly be considered as a CL task (Farquhar & Gal, 2018).

A.2 DOMAIN INCREMENTAL LEARNING (DOMAIN-IL)

Domain-IL refers to the CL scenario where the classes remain the same in each subsequent task but the input distribution changes. We consider **Rotated-MNIST** (Lopez-Paz & Ranzato, 2017) where each task contains digits rotated by a fixed angle between 0 and 180 degrees. We do not consider the related popular evaluation protocol **Permuted-MNIST** (Kirkpatrick et al., 2016) which applies a fixed random permutation to the pixels for each task as it violates the cross-task resemblance desiderata and deviates from the goal of continual learning (Farquhar & Gal, 2018). However, for completion, we provide the results on Permuted MNIST in supplementary.

A.3 GENERAL INCREMENTAL LEARNING (GIL)

The aforementioned CL scenarios fail to assimilate the challenges in the real world, setting where the task boundaries are blurry and the learning agent must rather learn from a continuous stream of data where classes can reappear and have different data distributions. The CL method must deal with the issues of sample efficiency, imbalanced classes, and efficient transfer of knowledge in addition to preventing catastrophic forgetting. To test the efficacy of our method in this challenging setting, we consider two GIL evaluation protocols. **MNIST-360** (Buzzega et al., 2020a) models a stream of data which presents batches of two consecutive MNIST images with each sample rotated at an increasing angle and the sequence is repeated three times. This exposes the model to both a sharp distribution shift when the class changes and a smooth rotational distribution shift. However, the number of classes in each task and the samples are uniform. The Generalized Class Incremental Learning (GCIL) (Mi et al., 2020) utilizes probabilistic modeling to sample the classes and data distributions in each task. Hence, the number of classes in each task is not fixed, the classes can overlap and the sample size for each class can vary. Following Mi et al. (2020), we use GCIL on CIFAR-100 (Krizhevsky et al., 2009) dataset (**GCIL-CIFAR-100**), set the number of samples

and maximum number of classes per task to 1000 and 50 respectively, number of tasks to 20, and evaluate on both uniform and longtail (imbalanced) sample distribution.

B Additional Results

In this section, we provide additional experimental results and analysis on the behavior of the model.

B.1 Permuted MNIST

We excluded the results on Permuted-MNIST from the main paper to discourage the use of this benchmark for evaluating the efficacy of continual learning methods. Since the permutations for each subsequent task are completely independent and random, they bear no resemblance with the previously learned tasks, and therefore as highlighted in Farquhar & Gal (2018), Permuted-MNIST provides an unrealistic best-case scenario for continual learning which directly affects how new tasks are learned. We provide the results, here, for the sake of completeness. Table S1 shows that similar to other datasets, CLS-ER proves effective under a lower memory budget for the buffer. For 5120 buffer size, CLS-ER performs on par with DER++.

JOINT	SGD	Buffer	ER	FDR	HAL	DER++	CLS-ER
94.33±0.17	40.70±2.33	200	72.37±0.87	74.77±0.83	74.15±1.65	83.58±0.59	**84.63±0.40**
		500	80.60±0.86	83.18±0.53	80.13±0.49	88.21±0.39	**88.30±0.14**
		5120	89.90±0.13	90.87±0.16	89.20±0.14	**92.26±0.17**	92.03±0.05

Table S1: Comparison with prior works on Perm-MNIST classification benchmark. The baseline results are from Buzzega et al. (2020a) and following them, we report the mean and one standard deviation over 10 runs.

Dataset	Buffer	Stable Model	Working Model	Plastic Model
S-MNIST	200	89.54±0.21	89.32±0.23	89.52±0.21
	500	92.05±0.30	91.61±0.47	92.04±0.33
	5120	95.73±0.10	95.65±0.15	95.73±0.12
S-CIFAR-10	200	66.19±0.75	50.09±1.48	62.68±1.94
	500	75.22±0.71	63.09±1.12	71.32±0.89
	5120	86.78±0.17	85.00±0.33	86.77±0.17
S-Tiny-ImageNet	200	21.95±0.26	9.72±0.41	16.72±1.78
	500	29.61±0.54	14.30±0.49	25.47±0.92
	5120	45.92±0.30	40.39±0.42	46.30±0.42
R-MNIST	200	92.26±0.18	89.37±0.47	89.99±0.43
	500	94.06±0.07	93.24±0.14	93.52±0.09
	5120	94.25±0.06	94.28±0.08	94.37±0.06
P-MNIST	200	84.63±0.40	84.33±0.45	84.54±0.41
	500	88.30±0.14	88.12±0.16	88.25±0.14
	5120	92.03±0.05	91.96±0.06	92.02±0.05
MNIST-360	200	66.37±0.83	55.59±1.74	60.60±1.41
	500	75.70±0.41	72.70±0.80	75.03±0.37
	1000	79.54±0.34	78.39±0.69	79.16±0.42
GCIL-CIFAR-100 (Uniform)	200	33.15±2.80	31.74±2.72	32.70±2.78
	500	37.01±1.67	35.89±1.69	36.18±1.68
	1000	41.09±1.58	40.44±1.80	40.70±1.66
GCIL-CIFAR-100 (Longtail)	200	29.57±3.80	28.19±3.90	29.12±3.89
	500	33.26±3.66	32.22±3.79	32.95±3.70
	1000	39.21±3.46	38.51±3.55	38.84±3.52

Table S2: CLS-ER components performance analysis for each of the experimental setting.

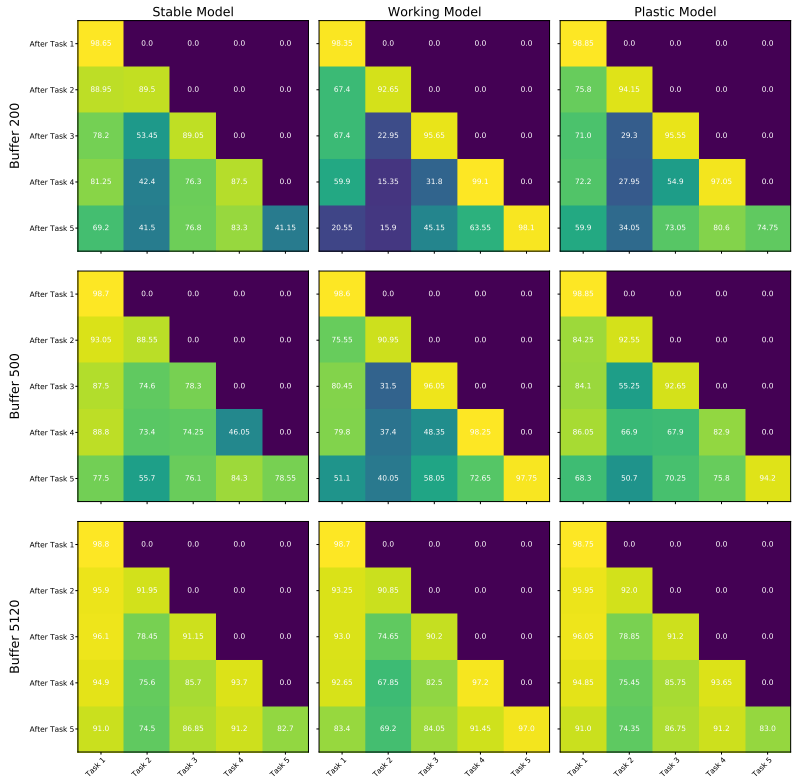

Figure S1: Test set task-wise performance for the individual models on S-CIFAR-10 with different buffer sizes. The task-wise performance (x-axis) is evaluated at the end of training of each task (y-axis) to evaluate how it is affected as training progresses.

B.2 CLS-ER Components Performance

CLS-ER involves the interplay between the working model and the two semantic memories: the plastic and stable models. While we use the stable model for final inference, here we provide the performance of each of these individual components to provide further insights into the workings of our method. Table S2 shows the corresponding performance of the working model and plastic model for each of our experimental settings. We can see that the stable model can effectively consolidate knowledge across the tasks and therefore provide the highest mean performance for the vast majority of the settings. Figures S1 and S2 further shows how the task-wise performance (on test set) of each of the component varies as subsequent tasks are learned. The stable model retains the performance on previous tasks while the plastic model adapts better to the recent task. Both these models provide feedback to the working model which in-turn improves the plastic and stable model.

B.3 Task Probabilities

With the same goal as with model calibration, we provide the task probabilities of the models trained with different buffer sizes on S-CIFAR-10 and S-Tiny-ImageNet. Figures S3 and S4 show that CLS-ER consistently achieves more uniform task probabilities compared to ER and DER++ and effectively mitigates the bias towards the last task.

B.4 Model Calibration

To further test the consistency of CLS-ER in providing well-calibrated models and the impact of the buffer size, we evaluate the calibration of models trained with different buffer sizes on S-CIFAR-10 and S-Tiny-ImageNet. Figures S5 and S6 show that CLS-ER consistently provides better calibrated models compared to ER and DER++. Remarkably, for both the datasets, on lower buffer sizes, the

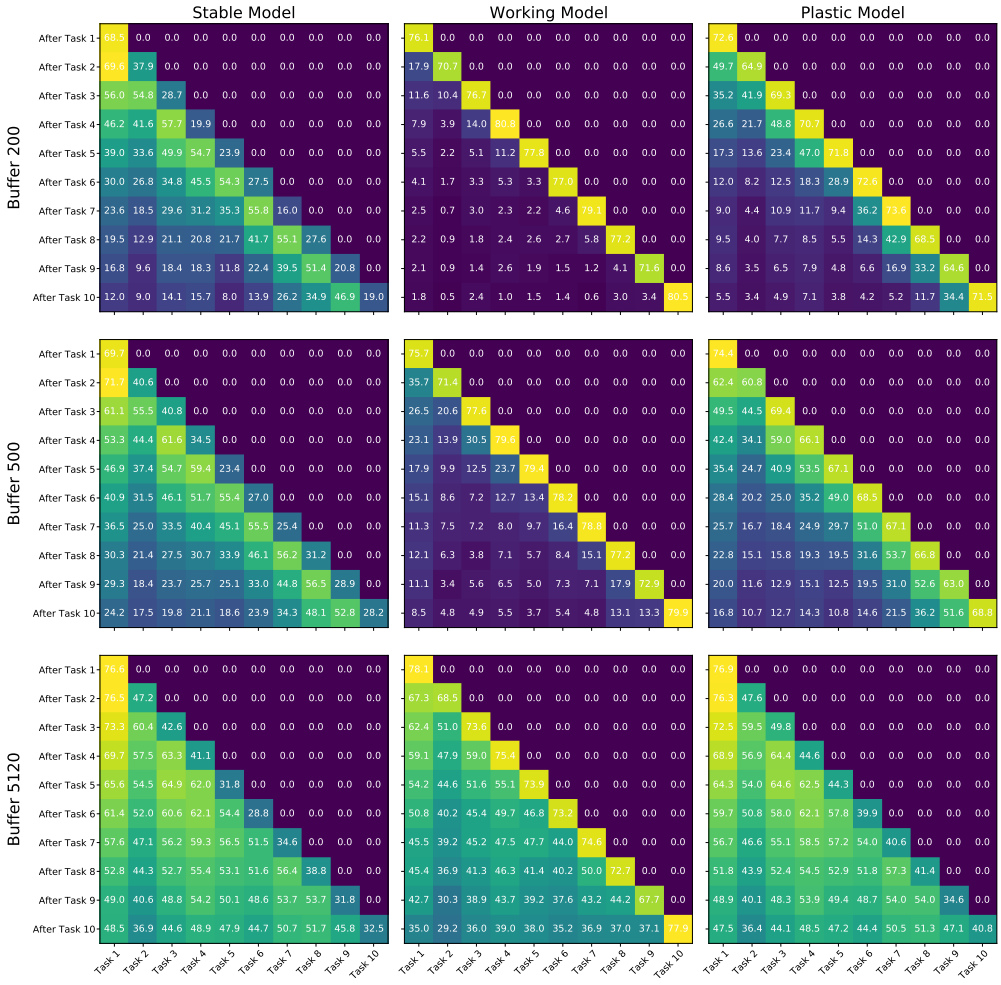

Figure S2: Test set task-wise performance for the individual models on S-Tiny-ImageNet with different buffer sizes. The task-wise performance (x-axis) is evaluated at the end of training of each task (y-axis) to evaluate how it is affected as training progresses.

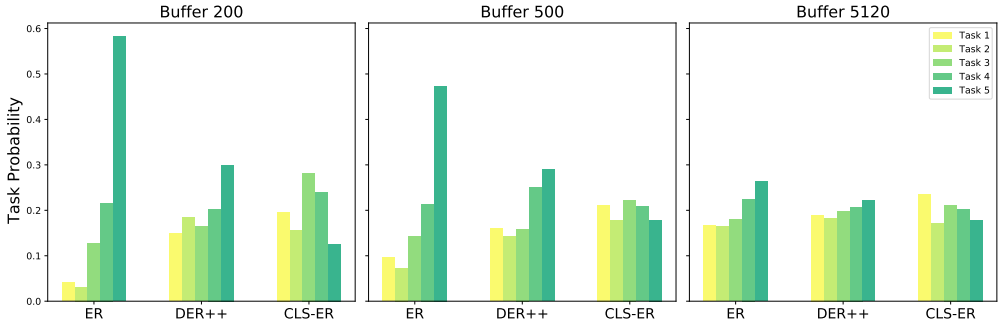

Figure S3: Task probabilities for different methods on S-CIFAR-10 with varying memory budget.

difference in Expected Calibration Error (ECE) is considerable. This demonstrates the capability of CLS-ER to train high-performance and reliable models under challenging conditions.

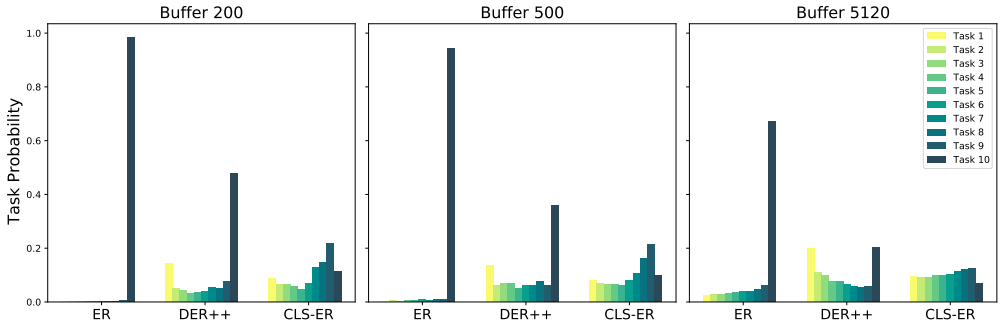

Figure S4: Task probabilities for different methods on S-Tiny-ImageNet with varying memory budget.

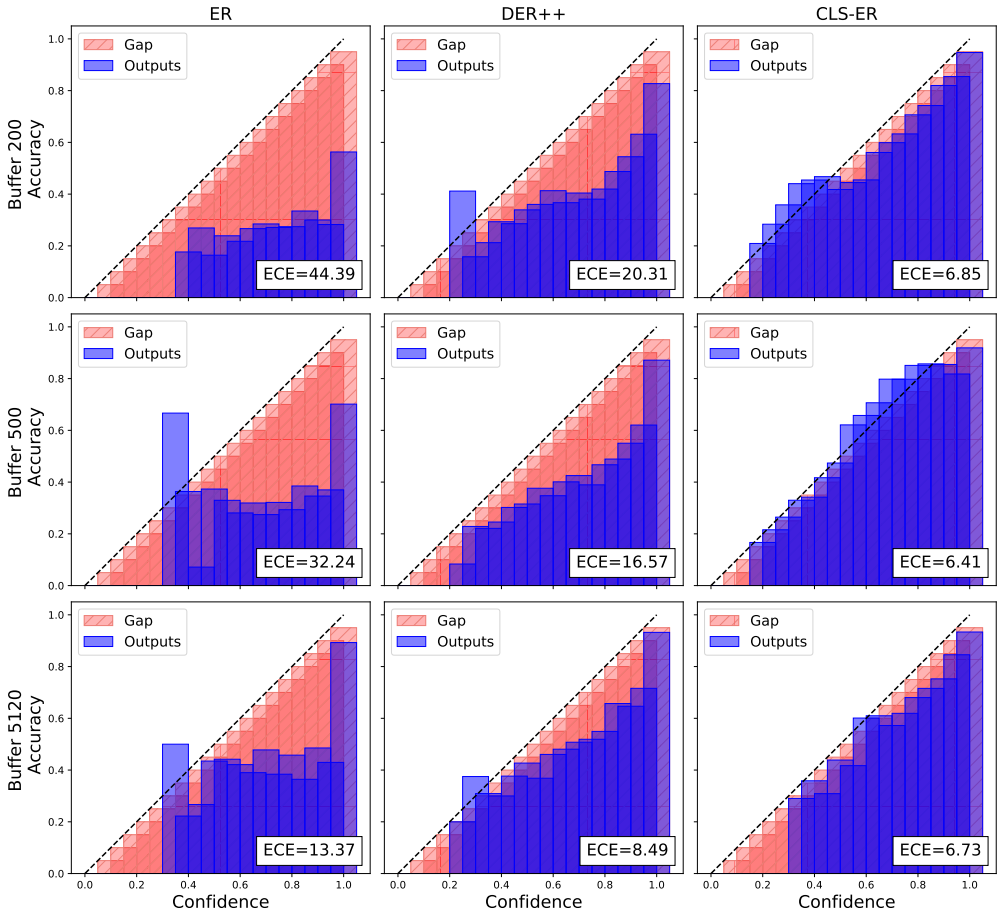

Figure S5: Reliability plots for the different methods on S-CIFAR-10 with varying memory budget.

B.5 Effect of Hyperparameters

The interaction between the three components of CLS-ER is complementary. Table S3 shows how the performance of each component is affected under different hyperparameter settings. We can draw the following conclusions from the results. The performance improvement in the plastic and stable model is reflected in the working model and the best performance is seen in cases where both the semantic memories are performing well (albeit the focus on tasks is different). This highlights the crucial role of both memories in enabling CLS-ER to learn efficiently. For a fixed r_S value,

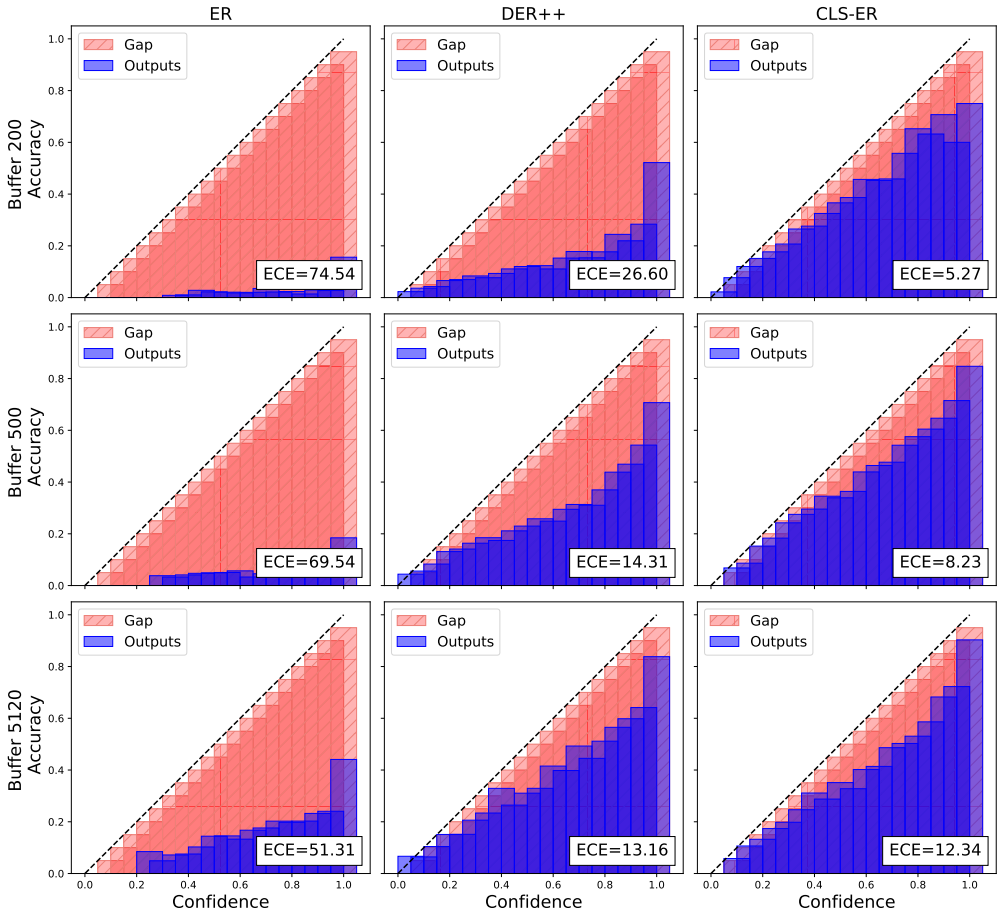

Figure S6: Reliability plots for the different methods on S-Tiny-ImageNet with varying memory budget.

the final performance of the stable model is affected considerably by the performance of the plastic model. The method is not highly sensitive to the particular choice of hyperparameters as different settings can attain similar performance. Because of the complementary nature of the components, we can often fix a set of parameters (e.g. λ, α_S, α_S and r_S) and only finetune the remaining parameters (e.g. r'_P) which facilitates hyperparameter tuning significantly.

C Training and Implementation Details

For a fair comparison between different CL methods and robust evaluation, it is important to test them under uniform experimental settings on the same CL scenarios. We, therefore, provide details of our implementation and experimental conditions along with the hyperparameters selected for each setting for reproducibility.

C.1 Implementation

We extended the Mammoth framework in PyTorch provided by Buzzega et al. (2020a) with our method and the GCIL-IFAR-100 dataset. *The code will be made publicly available*.

C.2 Hyperparameter Selection

For a fair comparison, we aim to keep the experimental settings close to the current state-of-the-art DER++ (Buzzega et al., 2020a) as much as possible to disassociate the effect of the training

schedule. We use the same optimizer, number of epochs, batch size, and memory batch size as DER++. For S-Tiny-ImageNet, we reduce the number of epochs to 50 from 100 used by DER++ as our method can learn efficiently with fewer epochs, and quickly acquiring new knowledge is preferred for CL. Similar to DER++, we finetune the memory batch size for S-MNIST and MNIST-360. We select the hyperparameters for each of the experimental setting using a small validation set, $\alpha_S, \alpha_P \in (0.99, 0.999)$, $r_S, r_P \in (0, 1]$, $\lambda \in (0, 2]$. Table S4 provides the hyperparameters used for each of the experimental settings. Note that for the vast majority of datasets, we use uniform settings (lr, epochs, batch size, memory batch size, and $lambda$) across the different buffer sizes and requires only slight modifications in the other hyperparameters which shows that our method does not require extensive finetuning for different memory budgets.

C.3 GCIL-CIFAR-100

To test our method under challenging GIL settings that better simulate the challenges of CL in the real world, we incorporate the GCIL setting from the code provided by Mi et al. (2020) with the continual dataset template class in the mammoth framework. We set the number of phases (length of task sequences) to 20, with the total number of samples in each phase set to 1000 and the maximum number of classes in each phase set to 50. We evaluate on both uniform and longtail (imbalanced) data distributions. Since GCIL involves the probabilistic sampling of the classes and their samples in each phase, the random seed determines the complexity of the GCIL setting. We use 10 different identical random seeds for our experiments so that each method is evaluated under identical settings and the difference between longtail and uniform is only the data distribution between the classes in each phase.

For each of our method, we use identical training scheme (lr=0.1, epochs=100, batch size=32 and memory batch size=32). For DER++, as per the authorts suggestion, we performed hyperparameter search over $\alpha \in [0.2, 0.3]$ and $beta \in [0.5, 1.0]$ with step size of 0.1. Table S5 provides the parameters chosen for each of the method under the different settings.

C.4 Perturbation Analysis

For the perturbation analysis, we used the code and checkpoints provided by Buzzega et al. (2020a) for DER++ and ER. We would like to express our gratitude to the authors for their support and for making the mammoth framework available for the research community which provides a framework for a fair comparison of different CL methods under uniform experimental conditions.

λ	r_S	r_P	Stable Model	Working Model	Plastic Model
0.1	0.1	0.2	73.53±1.07	62.80±0.63	71.11±2.21
		0.3	72.44±1.37	63.53±1.98	70.97±1.71
		0.4	73.05±0.93	61.81±1.92	68.75±2.20
		0.5	75.16±1.09	63.95±1.92	70.42±1.09
		0.6	75.04±0.66	62.82±0.70	69.61±0.31
		0.7	73.94±0.48	63.34±0.46	70.30±1.68
		0.8	74.61±1.10	62.68±0.65	70.74±0.39
		0.9	73.74±2.14	62.69±1.97	69.52±0.79
		1.0	75.73±0.68	64.21±1.11	72.00±0.56
	0.2	0.3	70.26±1.79	61.63±1.03	69.31±1.82
		0.4	71.80±1.17	62.64±0.18	70.64±1.22
		0.5	70.69±2.13	61.76±0.64	69.65±1.92
		0.6	72.45±0.68	63.87±0.85	71.29±0.72
		0.7	71.47±1.98	61.12±1.90	70.22±2.24
		0.8	72.16±0.56	62.71±0.57	70.83±0.64
		0.9	72.09±0.59	63.33±1.01	71.20±0.87
		1.0	72.05±1.35	63.74±1.75	71.01±1.28
	0.3	0.4	68.46±1.48	60.96±1.62	68.31±1.40
		0.5	70.05±2.54	63.06±1.26	69.90±2.57
		0.6	69.57±1.07	61.25±1.96	69.36±1.06
		0.7	68.99±2.34	61.61±2.17	68.81±2.27
		0.8	71.21±0.48	63.08±0.82	70.99±0.57
		0.9	71.26±1.47	62.33±0.64	71.03±1.56
		1	69.00±0.41	61.38±0.92	68.69±0.31
0.15	0.1	0.2	70.19±1.97	61.39±2.06	69.81±1.60
		0.3	73.72±0.83	62.07±0.84	70.18±0.09
		0.4	71.60±2.30	61.11±2.00	69.15±1.08
		0.5	74.18±0.37	63.32±0.98	71.08±2.04
		0.6	74.90±0.40	62.35±2.31	71.58±0.79
		0.7	74.52±1.10	62.59±2.64	70.90±2.30
		0.8	75.27±1.21	62.00±1.98	71.27±1.64
		0.9	74.61±0.91	63.47±1.60	70.49±0.95
		1.0	76.03±0.64	63.63±1.01	71.42±1.11
	0.2	0.3	72.59±1.44	61.81±1.03	72.02±1.30
		0.4	71.30±3.42	63.15±0.51	70.92±2.83
		0.5	69.89±1.95	60.60±0.95	68.87±2.56
		0.6	72.34±0.89	62.18±1.31	71.15±0.94
		0.7	72.70±1.11	62.50±1.18	71.49±1.21
		0.8	72.42±1.50	61.85±0.83	71.04±1.68
		0.9	71.18±0.71	61.81±1.29	70.09±0.54
		1.0	73.52±0.65	64.19±0.86	72.56±0.52
	0.3	0.4	70.32±1.39	62.39±2.00	70.13±1.33
		0.5	71.60±1.53	62.67±2.08	71.40±1.54
		0.6	70.36±1.82	62.28±2.28	70.13±2.03
		0.7	69.79±1.93	61.13±1.37	69.65±1.82
		0.8	69.85±0.95	60.69±1.63	69.78±0.60
		0.9	71.32±1.68	61.79±1.41	71.03±1.61
		1.0	71.39±0.49	62.35±0.88	71.11±0.55

Table S3: The effect of different hyperparameter settings on the individual components of CLS-ER trained on S-CIFAR-10 with 500 buffer size. For all the experiments α_S and α_P are fixed to 0.999 and the performance is averaged over 3 runs with different initialization.

Dataset	Buffer	lr	Epochs	Batch Size	Memory Batch Size	λ	α_S	α_P	r_S	r_P
S-MNIST	200	0.03	1	10	128	2.0	0.99	0.99	0.9	1.0
	500	0.1	1	10	32	2.0	0.99	0.99	0.9	1.0
	5120	0.1	1	10	32	2.0	0.99	0.99	0.8	1.0
S-CIFAR-10	200	0.1	50	32	32	0.15	0.999	0.999	0.1	0.3
	500	0.1	50	32	32	0.15	0.999	0.999	0.1	0.9
	5120	0.1	50	32	32	0.15	0.999	0.999	0.8	1.0
S-Tiny-ImageNet	200	0.1	50	32	32	0.1	0.999	0.999	0.04	0.08
	500	0.1	50	32	32	0.1	0.999	0.999	0.05	0.08
	5120	0.1	50	32	32	0.1	0.999	0.999	0.07	0.08
R-MNIST	200	0.2	1	128	128	0.75	0.999	0.99	1.0	1.0
	500	0.2	1	128	128	0.75	0.999	0.99	1.0	1.0
	5120	0.2	1	128	128	0.75	0.999	0.99	1.0	1.0
P-MNIST	200	0.2	1	128	128	1.0	0.99	0.99	0.8	1.0
	500	0.2	1	128	128	1.0	0.99	0.99	0.8	1.0
	5120	0.2	1	128	128	1.0	0.99	0.99	0.9	1.0
MNIST-360	200	0.2	1	16	16	0.75	0.999	0.99	1.0	1.0
	500	0.2	1	16	32	1.25	0.99	0.99	0.9	1.0
	1000	0.2	1	16	128	0.75	0.99	0.99	0.9	1.0

Table S4: The hyperparameters used for each of the experimental settings for CLS-ER.

Distribution	Method	Buffer	Parameters
Uniform	CLS-ER	200	$\lambda = 0.15$, $\alpha_S = 0.999$, $\alpha_P = 0.999$, $r_S = 0.6$, $r_P = 0.7$
		500	$\lambda = 0.15$, $\alpha_S = 0.999$, $\alpha_P = 0.999$, $r_S = 0.6$, $r_P = 0.9$
		1000	$\lambda = 0.15$, $\alpha_S = 0.999$, $\alpha_P = 0.999$, $r_S = 0.6$, $r_P = 0.8$
	DER++	200	$\alpha = 0.2$, $\beta = 0.5$
		500	$\alpha = 0.2$, $\beta = 0.6$
		1000	$\alpha = 0.3$, $\beta = 0.6$
Longtail	CLS-ER	200	$\lambda = 0.1$, $\alpha_S = 0.999$, $\alpha_P = 0.999$, $r_S = 0.6$, $r_P = 0.7$
		500	$\lambda = 0.1$, $\alpha_S = 0.999$, $\alpha_P = 0.999$, $r_S = 0.6$, $r_P = 0.7$
		1000	$\lambda = 0.1$, $\alpha_S = 0.999$, $\alpha_P = 0.999$, $r_S = 0.6$, $r_P = 0.8$
	DER++	200	$\alpha = 0.2$, $\beta = 0.6$
		500	$\alpha = 0.2$, $\beta = 0.8$
		1000	$\alpha = 0.3$, $\beta = 0.9$

Table S5: The hyperparameters used for GCIL-CIFAR-100 experiments. For each of the experiment, we used lr=0.1, epochs=100, betch size=32 and buffer memory batch=32.